Proceedings of ISFOG 2025
5TH INTERNATIONAL SYMPOSIUM ON
FRONTIERS IN OFFSHORE GEOTECHNICS
Nantes, France | June 9-13 2025

ISBN 978-2-85782-758-0

Investigation of the effect of scour protection systems on the stiffness of laterally loaded wind turbines

A. Kheffache*
Ghent University, Ghent, Belgium

B. Stuyts, C. Sastre Jurado
Ghent University, Ghent, Belgium

W. Weijtjens
VUB, Brussels, Belgium

*Anis.kheffache@ugent.be

ABSTRACT:
As a result of a growing demand for higher power output, offshore wind turbines are continuously growing in size (bigger rotor and monopile diameters) and mass (heavier rotor-nacelle assembly and support structure). Moreover, offshore wind farms are being installed in deeper waters, where the preferred type of supporting structure is still the monopile, which are expected to increase in length. As a result, the natural frequency of offshore wind turbines is expected to decrease towards the forcing wave frequency, raising concerns about dynamic amplification. On the other hand, monitoring data on offshore wind turbines shows a stiffer behaviour than expected, which was linked to the possible stiffening effects of scour protection systems, which could possibly be taken into account during design to justify a higher natural frequency of offshore wind turbines.

In this paper, the effect of the scour protection on the stiffness of a monitored wind turbine monopile subjected to lateral monotonic loading is investigated using 3D FEM analyses in ABAQUS. The scour protection's geometry is first established using bathymetric measurements around the studied wind turbine, and the properties such as the scour protection's unit weight and modulus are estimated. The scour protection is modelled using a simple Mohr-Coulomb law, while the soil medium is modelled using the hypoplastic models for sand and clay, which were calibrated in previous works. The wind turbine's FEM model is subjected to lateral loading, and the effect of the scour protection is quantified on the bending moment profiles along the monopile, as well as on the wind turbine's lateral stiffness.
Keywords: Offshore; geotechnics; wind energy; scour protection; stiffness.

1 INTRODUCTION

Offshore wind turbines are getting more attention, as the need for cleaner energy is being echoed worldwide. Monopiles; which are big-diameter hollow steel piles; are one of the main support structures for offshore wind turbines, as they form not less than 60% of the total installed foundations.

Previous works (Kheffache et al., 2024) highlighted a mismatch between the as-designed and as-built dynamics of offshore wind turbines. The mismatch was linked to the reduced stiffness of the simulated wind turbines when compared to the monitored ones. The missing stiffening contribution of the scour protection in the numerical models was suggested as one of the possible reasons.

In this work, the mismatch between the simulated and the monitored behaviour of offshore wind turbines is investigated, by using 3D FEM models which take into account the scour protection system.

2 SCOUR PROTECTION LITERATURE REVIEW

Scour consists of the global or local lowering of the seabed level. Scour is generally caused by the complex water flow at the seabed level, which is obstructed by the monopile structure.

Several authors have investigated the effect of scour and scour protection on the response of laterally loaded piles. Winkler et al. (2023) presented a case study where the 1st side-side natural frequency (bending mode) of a monitored wind turbine was tracked before, during, and after the installation of the scour protection system around a monopile-supported offshore high voltage station (OHVS) located in the Belgian North Sea. A clear increase in the wind turbine's natural frequency is observed post-installation, highlighting the increase in the lateral stiffness. More recently, Mayall et al. (2025) investigated the effect of scour protection based on previously carried reduced-scale

tests (Mayall et al., 2020). Similarly, it was found that the rock fill-type scour protection could contribute to the overall stiffness of offshore wind turbines, as it was possible to partially recover some of the lost resonance frequency due to scouring.

It has been identified that the scour protection system could increase the stiffness of offshore wind turbines through two mechanisms, the scour protection has a weight effect; which increases the effective stress of the supporting soil below, which in turn increases the stiffness of the soil (soil stiffness being stress dependant). The scour protection can also provide extra fixity for the wind turbine at the mudline level, through its modulus, shortening the free length of the monopile. The modulus effect is harder to quantify and more uncertain compared to the weight effect. The shear stiffness of the scour protection is expressed using the following equation:

$$G_{max} = B_{sp} p_{ref} \left(\frac{p'}{p_{ref}}\right)^{0.5} \qquad (1)$$

Where p_{ref} is a reference pressure set to 101 kPa, p' is the mean effective pressure and B_{sp} is a nondimensional factor. Mayall et al. (2025) used flume test experiments to determine the value of the B_{sp} factor, in order to numerically match the change in frequency of the instrumented pile. Two values of B_{sp} were derived, 259 and 500 that corresponds to an "as installed" and "post flow" scour protection states, the latter being the result of "sand accretion" inside the scour protection system. In an attempt to back-calculate the natural frequency on a real wind turbine (Mayall et al., 2025), which experienced scour, which was mitigated with a scour protection, it was noticed that the previously calibrated B_{sp} values from the flume experiments were not enough to restore all the lost stiffness, possibly implicating that higher values of B_{sp} could be applicable in-situ.

3 SITE CONDITIONS

3.1 Monopile

The studied wind turbine monopile is located in the Belgian North Sea. The monopile is monitored using different monitoring devices such as fibre Bragg Gratings (FBGs) that record the strains along the monopile at predefined depths. The wind turbine is also equipped with SCADA system that records the performance of the wind turbine. The monopile's geometry is given in the following table:

Table 1.Geometry of the monopile

h (m)	L (m)	t (mm)	Water depth (m)	D (m)
37	29.9	57-95	32	5

Where h is the stick-up length the, L is the embedded length ,t is the monopile's wall thickness and D is the monopile's diameter.

3.2 Soil

The monopile is embedded in a multilayered soil medium in which the top consists of an 8m thick medium-dense sand layer, and the bottom consists of a >40m thick clay layer that is heavily overconsolidated at the top. The cone tip resistance measured during cone penetration test at the exact wind turbine location is shown in Figure 1.

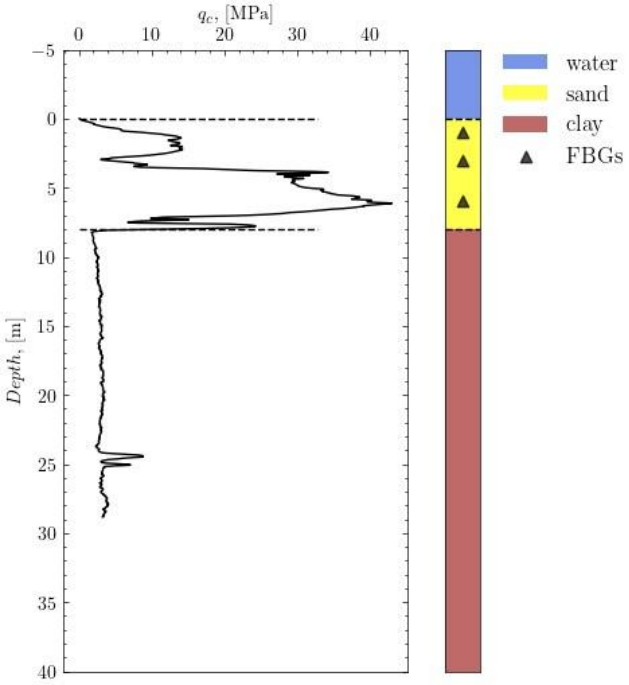

Figure 1. CPT, FBGs position, and soil layering at the wind turbine location.

3.3 Scour protection

The wind turbine that is being investigated in this work is surrounded by a scour protection system that was placed right after the monopile installation. The geometry of the scour protection (thickness and length) was extracted from the bathymetric surveys that were carried out before and after the installation of the scour protection system. The best-estimate scour protection geometrical characteristics are given in the following table:

Table 2. Geometry of the scour protection

h (m)	R_{top} (m)	R_{bot} (m)
1.5	13.375	17

Where h is the scour protection's thickness, R_{top} is the top radius and $R_{bot}$is the bottom radius.

4 MODELLING

The 3D FEM ABAQUS model is shown in Figure 2. Only half of the model is simulated, taking advantage of the symmetry in the y direction.

4.1 Loads

The quasi-static wind-induced loads were derived from the monitoring data during normal operational conditions of the wind turbines and were reported directly at the head of the monopile. A more detailed explanation is given in Kheffache et al. (2024). A total of 26 load cases were considered for this work.

4.2 Soil modelling

The sand and clay layers were modelled using the hypoplastic constitutive models for sand and clay (Mašín, 2013; von Wolffersdorff, 1996). These models were selected mainly due to the control that they confer over soil stiffness and it's degradation. The constitutive models were previously calibrated in other works (Kheffache et al., 2024).

4.3 Scour protection modelling

The scour protection layer was modelled using a simple Mohr-Coulomb model. Opting for a more advanced constitutive law would require more data which is not available. The "best-estimate" characteristics of the scour protection are given in the following table:

Table 3. Scour protection system's best estimate characteristics

$\varphi'(°)$	ν	B_{sp}	$\gamma'_{sp}(kN/m^3)$
40	0.3	500	11

Where φ' is the friction angle, ν is the Poisson's ratio, B_{sp} is a nondimensional parameter used to calculate the shear modulus G_{max} using Equation 1, selected according to Mayall et al. (2025) and γ'_{sp} is the effective unit weight, estimated using some scour protection parameters.

4.4 Interface modelling

The soil-pile interface is modelled using the ABAQUS general contact algorithm. The tangential contact was assigned a Mohr-Coulomb friction coefficient of 0.5, while the normal contact was assigned a "hard contact" behaviour.

Similarly, the pile-scour protection and soil-scour protection contact were modelled using the same strategy, a friction coefficient of 0.5 was also assigned (corresponding to a friction angle of 40 time a reduction coefficient of 0.66).

4.5 Parametric studies

Several parametric studies were carried out in this work, regarding the scour protection characteristics and geometry. Parametric analyses are first done on the weight effect then on the modulus effect. The best-estimate geometry and characteristics are given in Tables 2 and 3, the analyses that are performed are summarized in the following table:

Table 4. Summary of the parametric studies on scour protection

Parametric study	γ'_{sp}(kN/m^3)	Shear modulus (B_{sp})	Thickness (m)
γ'_{sp} (kN/m^3)	8, 11, 15	500	1.5
Thickness (m)	11	500	1, 1.5, 2
Shear Modulus (B_{sp})	11	260, 500, 750, 1000, 2200, 3000, 5000	1.5

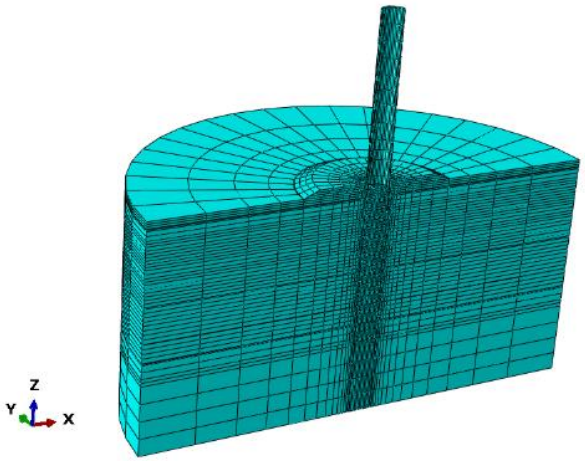

Figure 2. 3D FEM ABAQUS model of the monopile, soil and scour protection system.

5 RESULTS AND DISCUSSIONS

5.1 Increase of the soil's stiffness

The increase of the soil's stiffness in the top sand region under the weight of the scour protection (weight effect) is first quantified. The initial soil's stiffness profile G_{max} was interpreted from the CPT test shown

in Figure 1 using the Robertson & Cabal (2015) correlation (blue line in Figure 3). The interpreted stiffness profile is interpolated at several depths, taken at the centre of each mesh element using the following equation:

$$G_{max} = Ap_{ref}f(e)\left(\frac{p'}{p_{ref}}\right)^{0.5} \qquad (2)$$

Where p_{ref} is a reference pressure set to 101 kPa, p' is the mean effective pressure and A is a scaling factor. The void ratio function $f(e)$ is given by:

$$f(e) = \frac{(2.97-e)^2}{1+e} \qquad (3)$$

Where e is the void ratio. The A parameter value is calculated in order to match the stiffness profile (blue line) using Equation 2, the resulting interpolated stiffness profile is shown in circular black lines, the corresponding A parameter at each depth is also shown on the same figure. The stresses induced by the scour protection $p'_{soil+sp}$ are extracted from the 3D FEM model and are used to calculate a new stiffness profile using the previously calculated A parameter. The new G_{max} profile is shown in Figure 3 (pink crosses). The previously calibrated constitutive models are recalibrated to take into account the increased stiffness. All the coming analyses are by extracting a stress profile induced by scour protection, computing the increase in soil stiffness, and using it in a new analysis. It should be pointed out that no changes in void ratio were considered, and the increase of stiffness in the clay layer was not taken into account (minimal).

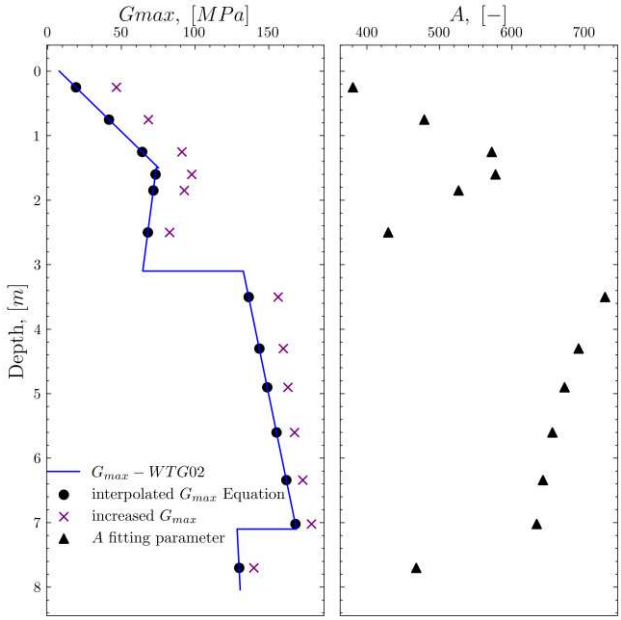

Figure 3. Quantification of the increase in soil stiffness caused by the scour protection's best-estimate weight and thickness.

5.2 Bending moments

The monitored and simulated bending moment profiles corresponding to the highest monitored load case are shown in Figure 4, considering different scenarios. The bending moments are normalized by the same highest moment value, which is found on the moment profile corresponding to the "no sp" scenario (purple curve in Figure 4). It can be seen that in all the considered scenarios, the simulated bending moments are higher than the monitored ones. Taking the scour protection into account shifts the bending moment profiles to the left (decrease) towards the monitored values, with a more pronounced shift when considering the scour protection modulus effect (B_{sp} of 500) on top of the weight effect (γ'_{sp} of 11 kN/m^3).

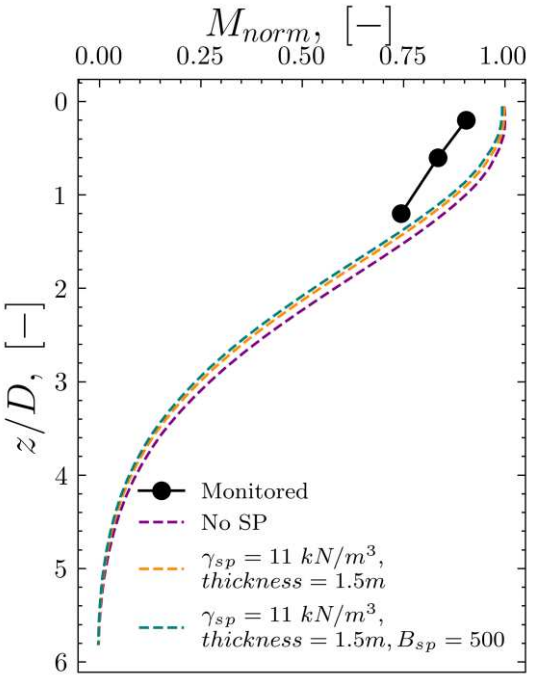

Figure 4.Monitored and simulated bending moments, considering different scour protection scenarios

The mismatch between the monitored and computed bending moments at each sensor depth (Figure 1) is quantified using the mean relative error (MRE), which is defined using the following equation:

$$MRE_M = \frac{1}{n}\sum_{i=0}^{n-1}\frac{M_m^{z,i} - M_s^{z,i}}{M_m^{z,i}} \qquad (4)$$

where $M_m^{z,i}$ and $M_s^{z,i}$ are the monitored and simulated moments at sensor depth z for the i-th load case, and n is the total number of load case (26 in this work). Negative and positive values of MRE translate into an over estimation and underestimation of the simulated bending moments compared to the monitored ones respectively. The MRE values are shown in Figure 5. The initial MRE values (without scour protection effects) are of -7.04, -17.8, and -12.19% at normalized depths of 0.2, 0.6 and 1.2 respectively. The MRE values drop to -6.7, -16.22 and -8.2% at the same normalized depths, when considering the weight effect of the scour protection only (unit weight and thickness). The MRE values drop even further to -6.13, -14.94 and -6% when including a scour protection modulus that corresponds to B_{sp} of 500 (Equation 1).

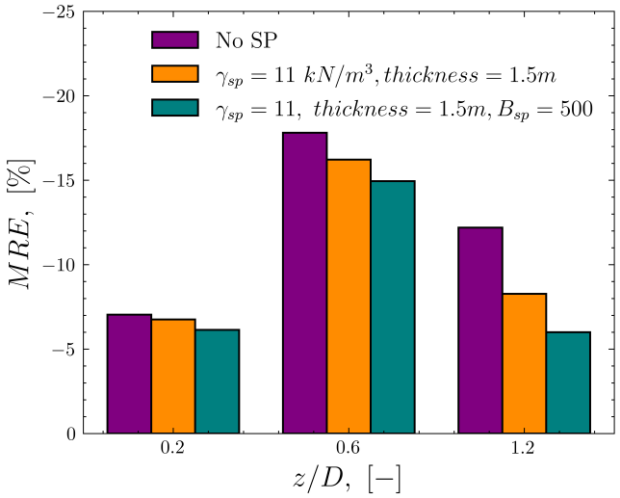

Figure 5. MRE at each normalized sensor depth, considering multiple scour protection scenarios.

The GMRE value; which is defined as the mean of the MRE values that were calculated at each sensor depth; is used to obtain a single value to quantify the mismatch between the simulated and monitored bending moments. The GMRE is used to investigate the combined effect of scour protection unit weight γ'_{sp} and thickness, without the modulus effect. The scour protection's pressure that is applied on the soil is calculated as $\gamma'_{sp} * thickness$. It can be seen from Figure 6 that GMRE decreases with an increasing scour protection pressure. This is indeed expected as an increase in pressure would lead to an increased effective stress profile and thus an increased soil stiffness. The GMRE that corresponds to the best-estimate γ'_{sp} and thickness of 11 kN/m^3 and 1.5m respectively, is shown with a red circle in Figure 6 and has a value of -10.4%, which is a reduction of 1.93% from the GMRE value without scour protection of -12.34% (applied pressure of 0).

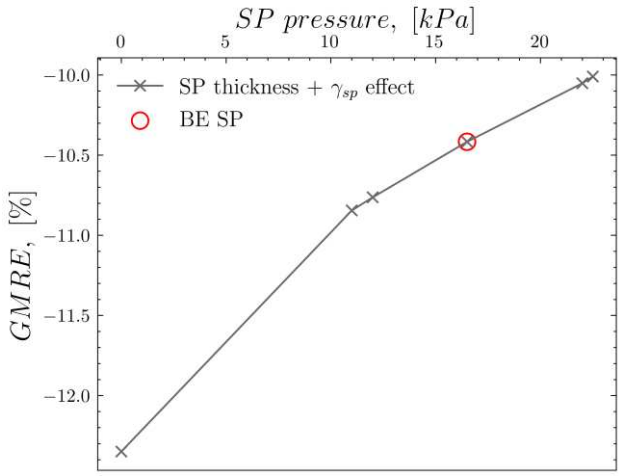

Figure 6. GMRE values considering different scour protection applied pressures on the soil.

The effect of scour protection's modulus is then investigated. Since the weight effect is more probable than the modulus effect, it was decided to include their contribution when studying the modulus effect. The results are shown in Figure 7. It can be seen that an increase of modulus decreases the GMRE values, which seem to plateau at higher scour protection G_{max} values. The GMRE value that corresponds to the best estimate scour protection characteristics ($\gamma'_{sp} = 11\ kN/m^3$, thickness 1.5m and $B_{sp} = 500$) is of -9.02%, which is a reduction of 3.32% compared to the case without scour protection and 1.39% compared to the best-estimate weight effect. The contribution from the best-estimate scour protection characteristics without modulus is shown in red dashed lines, which allows the visualisation of the "pure" modulus contribution shown in blue.

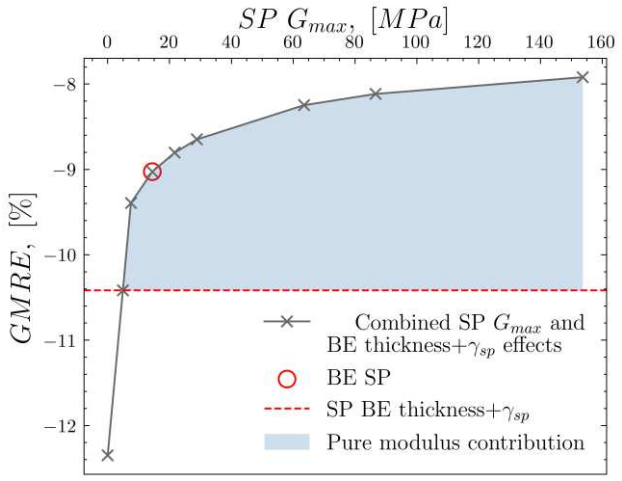

Figure 7. GMRE values considering a best estimate $\gamma'_{sp} = 11\ kN/m^3$ and a thickness of 1.5m, in combination with different scour protection modulus values.

It can be seen that although the scour protection reduces the mismatch, a fairly significant amount of

GMRE is still present, which indicates that the mismatch is due to multiple concurrent reasons, such as installation effects, cyclic effects on soil stiffness and the uncertainty on the initial soil stiffness correlation from CPT tests.

5.3 Stiffness

The effect of the scour protection system on the lateral rotational stiffness of the wind turbine monopile is further investigated.

The rotational stiffness is defined according to the following equation:

$$K_\theta = \frac{M}{\theta} \qquad (5)$$

where M is the moment at mudline level that corresponds to a very small pile rotation at mudline level θ. Similarly to Figure 6, Figure 8 shows the effect of scour protection applied pressure on the lateral stiffness of the studied wind turbine. The rotational stiffness increases with an increase of applied pressure which gives rise to an increase in soil stiffness. The increase in rotational stiffness that corresponds to the best estimate scour protection γ'_{sp} and thickness is of 6.6% when compared to a rotational stiffness without scour protection.

When investigating the effect of scour protection modulus on K_θ combined with the best estimate γ'_{sp} and thickness, it can be seen from Figure 9 that the increase of K_θ seems to have a similar plateau as the decrease of GMRE in Figure 7. The increase that corresponds to the best estimate scour protection characteristics ($\gamma'_{sp} = 11\ kN/m^3$, thickness 1.5m and $B_{sp} = 500$) compared to the $K_\theta^{No\ SP}$ (0 applied pressure) is of 11.2%, the increase compared to the best estimate γ'_{sp} and thickness (without modulus) is of 4.6%. The pure scour protection modulus contribution is also shown in blue. The reduction in GMRE (which is essentially a reduction in the simulated bending moment) is in fact caused by the increase in the lateral stiffness of the wind turbine, which was already established in previous works (Kheffache et al., 2024).

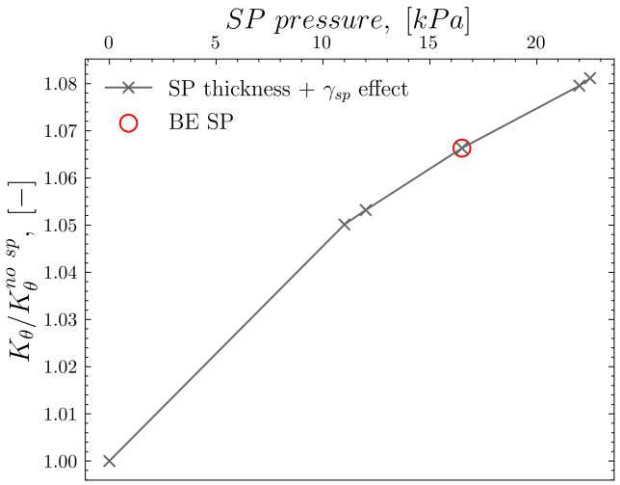

Figure 8. Normalized rotational stiffness values considering different scour protection applied pressures on the soil.

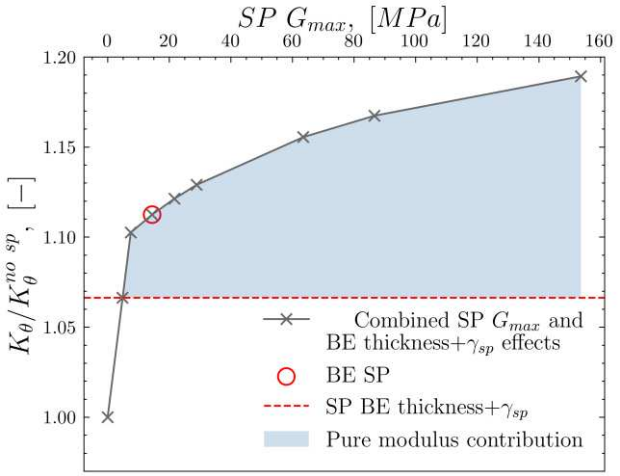

Figure 9. Normalized rotational stiffness values considering a best estimate $\gamma'_{sp} = 11\ kN/m^3$ and a thickness of 1.5m, in combination with different scour protection modulus values.

6 CONCLUSIONS, RECOMMENDATIONS AND FUTURE WORK

In this work, the effect of scour protection on bending moments and the lateral rotational stiffness of a monitored wind turbine monopile was investigated. Two mechanisms that can lead to an increase of the wind turbine's stiffness were studied: the weight effect and the modulus effect. The findings can be summarized as follows:

- The scour protection can increase the stiffness of laterally loaded wind turbines through two mechanisms, it increases the stiffness of the supporting soil by increasing the stress level, it also adds extra fixity at the mudline level, reducing the free length of the monopile.
- The weight effect of scour protection reduces the mismatch between the simulated and mon-

itored bending moments, as it increases the lateral stiffness. The decrease in the mismatch is further enhanced when taking into account the modulus effect.

The mismatch decrease seems to plateau, leaving the room for further possible reasons to it, such as installation effects, which might contribute to an increase in stiffness.

AUTHOR CONTRIBUTION STATMENT

A. Kheffache: Formal Analysis, Writing- Original draft, Software, Methodology. **B. Stuyts**: Supervision, Data curation. **C. Sastre Jurado**: Data curation. **W. Weijtjens**: Project administration

ACKNOWLEDGEMENTS

The authors would like to acknowledge the support of the Belgian Ministry of Economic Affairs through the EFT project WINDSOIL project. The Support of VLAIO through the De Blauwe Cluster SBO SOILTWIN project is also acknowledged.

REFERENCES

Kheffache, A., Stuyts, B., Sastre Jurado, C., Weijtjens, W., Devriendt, C., & Troch, P. (2024). Advanced simulations of monitored wind turbine monopiles located in the Belgian North Sea under operational quasi-static loading. Ocean Engineering, 311, 118914. https://doi.org/10.1016/j.oceaneng.2024.118914

Mašín, D. (2013). Clay hypoplasticity with explicitly defined asymptotic states. Acta Geotechnica, 8(5), 481–496. https://doi.org/10.1007/s11440-012-0199-y

Mayall, R. O., Burd, H. J., McAdam, R. A., Byrne, B. W., Whitehouse, R. J. S., Heald, S. G., & Slater, P. L. (2025). Numerical Modeling of the Influence of Scour and Scour Protection on Monopile Dynamic Behavior. Journal of Waterway, Port, Coastal, and Ocean Engineering, 151(1), 04024019. https://doi.org/10.1061/JWPED5.WWENG-2027

Mayall, R. O., McAdam, R. A., Whitehouse, R. J. S., Burd, H. J., Byrne, B. W., Heald, S. G., Sheil, B. B., & Slater, P. L. (2020). Flume Tank Testing of Offshore Wind Turbine Dynamics with Foundation Scour and Scour Protection. Journal of Waterway, Port, Coastal, and Ocean Engineering, 146(5), 04020033. https://doi.org/10.1061/(ASCE)WW.1943-5460.0000587

Robertson, P., & Cabal, K. L. (2015). Guide to Cone Penetration Testing. R:\Zotero\CA Technical references\2015 Robertson and Cabal - Guide to Cone Penetration Testing.pdf

von Wolffersdorff, P.-A. (1996). A hypoplastic relation for granular materials with a predefined limit state surface. Mechanics of Cohesive-Frictional Materials, 1(3), 251–271. https://doi.org/10.1002/(SICI)1099-1484(199607)1:3<251::AID-CFM13>3.0.CO;2-3

Winkler, K., Weil, M., Sastre Jurado, C., Stuyts, B., Weijtjens, W., & Devriendt, C. (2023). Quantifying the effect of rock armour scour protection on eigenfrequencies of a monopile supported OHVS. Journal of Physics: Conference Series, 2626, 012039. https://doi.org/10.1088/1742-6596/2626/1/012039